

# Persistent Sampling: Unleashing the Potential of Sequential Monte Carlo

 **Minas Karamanis**<sup>1,2\*</sup>

 **Uroš Seljak**<sup>1,2</sup>

<sup>1</sup>Berkeley Center for Cosmological Physics, University of California, Berkeley, CA 94720, USA

<sup>2</sup>Lawrence Berkeley National Laboratory, 1 Cyclotron Road, Berkeley, CA 94720, USA

## Abstract

*Sequential Monte Carlo* (SMC) methods are powerful tools for Bayesian inference but suffer from requiring many particles for accurate estimates, leading to high computational costs. We introduce *persistent sampling* (PS), an extension of SMC that mitigates this issue by allowing particles from previous iterations to persist. This generates a growing, weighted ensemble of particles distributed across iterations. In each iteration, PS utilizes multiple importance sampling and resampling from the mixture of all previous distributions to produce the next generation of particles. This addresses particle impoverishment and mode collapse, resulting in more accurate posterior approximations. Furthermore, this approach provides lower-variance marginal likelihood estimates for model comparison. Additionally, the persistent particles improve transition kernel adaptation for efficient exploration. Experiments on complex distributions show that PS consistently outperforms standard methods, achieving lower squared bias in posterior moment estimation and significantly reduced marginal likelihood errors, all at a lower computational cost. PS offers a robust, efficient, and scalable framework for Bayesian inference.

**Keywords:** sequential Monte Carlo, importance sampling, marginal likelihood.

## 1 Introduction

*Sequential Monte Carlo* (SMC) methods have emerged as powerful tools for tackling *Bayesian inference* problems in diverse scientific and engineering fields (Chopin, 2002; Del Moral et al., 2006; Chopin and Papaspiliopoulos, 2020). Their adaptive nature and inherent parallelizability make them attractive for navigating complex, multimodal, and non-linear posterior landscapes (Cappé et al., 2007). However, despite their strengths, standard SMC approaches face limitations associated with computational cost and efficiency.

SMC operates by propagating a population of particles through a sequence of intermediate probability distributions, interpolating between a chosen reference distribution (often the prior in Bayesian inference) and the target distribution (often the posterior). This sequence of targets can be constructed by “data annealing,” where observations are gradually introduced (i.e.,

---

\*mkaramanis@berkeley.edu

state-space models), or “temperature annealing,” where the influence of the likelihood function is progressively increased through an effective temperature parameter (Neal, 2001).

To transfer particles from one intermediate distribution to the next, SMC relies on three steps: *reweighting*, *resampling*, and *moving* (Chopin and Papaspiliopoulos, 2020). Reweighting utilizes importance sampling to adjust particle weights based on the agreement between the previous with the current intermediate distribution, guiding the population towards higher probability regions. Resampling then selectively discards low-weight particles and replicates high-weight ones. Finally, the moving step utilizes a Markov kernel to propose transitions for each particle within the current distribution, facilitating the exploration of the current target (Metropolis et al., 1953). Notably, the moving step is often the most computationally expensive one, but calculations for each particle are readily parallelizable (Lee et al., 2010). Furthermore, as a valuable byproduct, SMC algorithms estimate the marginal likelihood (model evidence), crucial for model comparison.

Despite its advantages, SMC suffers from inherent limitations. These stem from the limited and fixed size of the particle ensemble. The computational cost scales approximately linearly with the number of particles, often prompting a trade-off between accuracy and computational feasibility. Consequently, high-variance estimates plague both marginal likelihoods and posterior distributions. Another challenge lies in post-resampling particle correlation, where many identical particles remain after resampling, necessitating lengthy *Markov chain Monte Carlo* (MCMC) runs for diversification during the moving step.

To address these limitations, we introduce *persistent sampling* (PS), an extension of standard SMC that retains particles from past iterations. This method represents the current target distribution with an growing, weighted collection of particles accumulated over iterations. By treating particles from all previous iterations as samples from a mixture distribution, PS constructs a more diverse and rich sample of the target posterior without additional computational cost. Leveraging information from all iterations rather than just the last one, PS achieves significantly lower variance estimates for the marginal likelihood, enhancing model comparison accuracy. The resampled particles in PS are naturally decorrelated and distinct, reducing the need for extensive MCMC runs for diversification and thereby increasing efficiency.

The idea of using a mixture distribution to perform importance sampling in order to achieve lower-variance estimates was first proposed as the *balance heuristic* in multiple importance sampling (MIS) in the context rendering computer graphics (Veach and Guibas, 1995; Veach, 1998). Owen and Zhou (2000) showed that the balance heuristic of Veach and Guibas (1995) matches the deterministic mixture sampling algorithm of Hesterberg (1995). Since then, MIS with a mixture distribution has been utilized to improve the performance of many adaptive importance sampling (AIS) methods used for general Bayesian computation (Bugallo et al., 2017). Adaptive multiple importance sampling (AMIS) was the first AIS method to optimally recycle all past simulations using the aforementioned mixture approach (Cornuet et al., 2012). MIS has also been utilized to improve the sampling efficiency of population Monte Carlo (PMC), a subclass of AIS methods (Elvira et al., 2017; Elvira and Chouzenoux, 2022). More broadly, the idea of resampling

$N$  particles from a much larger pool also appears in the context of waste-free SMC (Dau and Chopin, 2022). However, waste-free SMC follows a different approach by resampling  $N$  particles from their respective Markov chains instead of past SMC iterations. Finally, in an attempt to utilize the particles of the intermediate distributions to enhance posterior estimates, several recycling techniques have been introduced (Nguyen et al., 2014). In this context, recycling acts as a post-processing step after sampling with SMC is completed, where particles from all intermediate distributions are reweighted to target the posterior.

The rest of this paper is organized as follows: Section 2 provides the necessary background, including a detailed description of the standard SMC algorithm and recycling post-processing procedures. Section 3 introduces the method following the construction of the PS algorithm. Section 4 presents numerical results, demonstrating the superior empirical performance of PS. Finally, Section 5 offers a summary and discussion of the main results, possible limitations, and potential extensions of the algorithm.

## 2 Background

Bayesian inference relies on Bayes' theorem, which mathematically expresses how a subjective degree of belief, or *prior probability distribution*  $\pi(\theta) \equiv P(\theta|\mathcal{M})$ , is updated given data,  $D$ , to form the *posterior probability distribution*  $\mathcal{P}(\theta) \equiv P(\theta|D, \mathcal{M})$  (Jaynes, 2003; MacKay, 2003). Here,  $\mathcal{M}$  is the model with parameters  $\theta$ . This theorem is captured by the equation

$$\mathcal{P}(\theta) = \frac{\mathcal{L}(\theta)\pi(\theta)}{\mathcal{Z}} \quad (1)$$

where  $\mathcal{L}(\theta) \equiv P(D|\theta, \mathcal{M})$  is the *likelihood function*, representing the probability of observing the data as a function of the parameters  $\theta$ , and  $\mathcal{Z} \equiv P(D|\mathcal{M})$  is the *model evidence* or *marginal likelihood*, that is, the probability of observing the data under the model. The strength of Bayesian inference lies in its formal framework for incorporating prior knowledge and systematically updating this knowledge in light of new data. Typically, the likelihood,  $\mathcal{L}(\theta)$ , and the prior,  $\pi(\theta)$ , are known and one seeks to estimate the posterior,  $\mathcal{P}(\theta)$ , and the evidence,  $\mathcal{Z}$ .

### 2.1 Sequential Monte Carlo

SMC propagates a set of  $N$  particles,  $\{\theta_t^i\}_{i=1}^N$ , through a sequence of probability distributions,  $p_t(\theta)$  for  $t = 1, \dots, T$ . This is achieved through the repeated application of a series of reweighting, resampling, and moving steps that are described in detail below. The SMC pseudocode is presented in detail in Algorithm 1.

The sequence of probability distributions,  $p_t(\theta)$  for  $t = 1, \dots, T$ , is generally chosen such that  $p_1(\theta)$  corresponds to a reference distribution from which sampling is straightforward, and  $p_T(\theta)$  corresponds to the generally intractable target distribution that we aim to approximate. In

the context of Bayesian inference, we typically focus on a *temperature annealing* sequence of the form

$$p_t(\theta) = \frac{\mathcal{L}^{\beta_t}(\theta)\pi(\theta)}{\mathcal{Z}_t} \quad (2)$$

that interpolates between the prior  $p_1(\theta) = \pi(\theta)$  and posterior distribution  $p_T(\theta) = \mathcal{P}(\theta) = \mathcal{L}(\theta)\pi(\theta)/\mathcal{Z}_T$  given a sequence of temperature values  $0 = \beta_1 < \dots < \beta_t < \dots < \beta_T = 1$  (Neal, 2001).

### 2.1.1 Reweighting

The reweighting step involves using importance sampling (IS) to weigh particles drawn from the previous distribution,  $p_{t-1}(\theta)$ , to target the current distribution,  $p_t(\theta)$  (Del Moral et al., 2006). The weights are defined as

$$W_t^i = \frac{p_t(\theta_{t-1}^i)}{p_{t-1}(\theta_{t-1}^i)} = \frac{\mathcal{Z}_{t-1}}{\mathcal{Z}_t} w_t^i, \quad (3)$$

where  $w_t^i$  are the unnormalized weights given by

$$w_t^i = \mathcal{L}(\theta_{t-1}^i)^{\beta_t - \beta_{t-1}}. \quad (4)$$

Assuming sufficient overlap between  $p_{t-1}(\theta)$  and  $p_t(\theta)$ , the weighted set of particles  $\{\theta_{t-1}^i, W_t^i\}_{i=1}^N$  should be distributed according to  $p_t(\theta)$ . The unknown ratio of normalizing constants in Eq. 3 can be estimated as

$$\frac{\mathcal{Z}_t}{\mathcal{Z}_{t-1}} = \frac{1}{N} \sum_{i=1}^N w_t^i, \quad (5)$$

where the weights  $w_t^i$  are given by Eq. 4. In the context of Bayesian inference, the reference distribution is chosen to be the prior  $\pi(\theta)$  with  $\mathcal{Z}_1 = 1$ , further simplifying calculations. In this case,  $\mathcal{Z}_T$  corresponds to the model evidence,  $\mathcal{Z} = p(d|\mathcal{M})$  (i.e., marginal likelihood), for a model,  $\mathcal{M}$ , and is crucial in the task of *Bayesian model comparison*.

In order to ensure the low variance of the weights  $\{W_t^i\}_{i=1}^N$  and the expected values constructed based on them, the temperature level  $\beta_t$  is typically determined adaptively. This is achieved by approximately maintaining a specified *effective sample size* (ESS), estimated as

$$\text{ESS}_t = \frac{(\sum_{i=1}^N w_t^i)^2}{\sum_{i=1}^N (w_t^i)^2} = \frac{1}{\sum_{i=1}^N (W_t^i)^2}. \quad (6)$$

ESS is maximized when the weight distribution is uniform, in which case  $\text{ESS} = N$  (Kong et al., 1994; Jasra et al., 2011). More formally,  $\beta_t$  is determined as

$$\beta_t = \inf_{\beta \in [\beta_{t-1}, 1]} \{\text{ESS}_t \geq \alpha N\}, \quad (7)$$

where values of  $\alpha$  typically range from 0.5 to 0.999, depending on the specific requirements of the inference task. Eq. 7 is commonly solved numerically using the bisection method (Arfken et al., 2011). Higher values of  $\alpha$  lead to a finer sequence of temperature levels and generally more robust results, albeit more computationally expensive. SMC typically terminates when  $\beta_t$  becomes 1, corresponding to the target posterior distribution. Using Eq. 7 to determine  $\beta_t$  is a form of adaptation and can incur a level of bias in the final results. Despite this, the introduced bias is often negligible and the estimates remain consistent (Moral et al., 2012; Beskos et al., 2016), rendering the use of Eq. 7 a standard practice in the field.

### 2.1.2 Resampling

Following the reweighting step, the particles,  $\{\theta_{t-1}^i\}_{i=1}^N$ , are resampled with probabilities proportional to their weights,  $\{W_t^i\}_{i=1}^N$  (i.e., multinomial resampling). The aim of this procedure is to eliminate particles with low weights and replicate the ones with high weights. Different resampling methods, such as multinomial and systematic resampling, with varying theoretical characteristics have been proposed to perform this step (Li et al., 2015; Gerber et al., 2019).

### 2.1.3 Moving

In SMC, after resampling, the particles undergo diversification through a sequence of MCMC steps to explore the distribution  $p_t(\theta)$ . The choice of MCMC kernel,  $\mathcal{K}_t$ , varies based on application-specific needs. For high-dimensional scenarios, gradient-based kernels like *Metropolis-adjusted Langevin algorithm* (MALA) or *Hamiltonian Monte Carlo* (HMC) are effective (Grenander and Miller, 1994; Rossky et al., 1978; Roberts and Tweedie, 1996; Roberts and Rosenthal, 1998; Duane et al., 1987; Neal, 2011). In contrast, low-to-moderate dimensional, non-differentiable problems may benefit from gradient-free approaches such as *random-walk Metropolis* (RWM) or *slice sampling* (SS) (Metropolis et al., 1953; Neal, 2003). *Independence Metropolis-Hastings* (IMH) kernels are also useful in certain low-dimensional cases (South et al., 2019). Additionally, machine learning-assisted methods like preconditioned MCMC have shown promise for highly correlated targets (Karamanis et al., 2022).

While the list of potential algorithms is not exhaustive, a key advantage of SMC is leveraging the empirical particle distribution to create effective MCMC proposals, contrasting with methods like *parallel tempering* (PT) that lack such auxiliary information (Swendsen and Wang, 1986; Geyer et al., 1991). One common strategy involves using the empirical covariance matrix of particles for RWM or as the mass matrix in MALA and HMC (Chopin, 2002). Examples of advanced applications include using a copula-based model calibrated on particle distribution for IMH, or employing normalizing flows trained on particle distribution for preconditioned MCMC (South et al., 2019; Karamanis et al., 2022). Furthermore, the MCMC kernel's hyperparameters, such as the proposal scale or mass matrix, can be fine-tuned using the mean Metropolis acceptance rate from the previous iteration.

---

**Algorithm 1:** Sequential Monte Carlo

---

**Data:** Number of particles  $N$ , ESS fraction  $\alpha$ , prior density  $\pi(\theta)$ , likelihood function  $\mathcal{L}(\theta)$ , Markov kernel  $\mathcal{K}_t$  with invariant density  $p_t(\theta)$

**Result:** Samples  $\{\theta_T^i\}_{i=1}^N$  from  $\mathcal{P}(\theta) = \mathcal{L}(\theta)\pi(\theta)/\mathcal{Z}$  and marginal likelihood estimate  $\mathcal{Z} \equiv \mathcal{Z}_T$

$t \leftarrow 1, \beta_t \leftarrow 0, \mathcal{Z}_1 \leftarrow 1;$

**for**  $i \leftarrow 1$  **to**  $N$  **do**

$\theta_1^i \sim \pi(\theta);$  /\* Sample prior distribution \*/

**while**  $\beta_t < 1$  **do**

$t \leftarrow t + 1;$

$\beta_t \leftarrow \inf_{\beta \in [\beta_{t-1}, 1]} \{\text{ESS}_t \geq \alpha N\};$  /\* Update temperature \*/

**for**  $i \leftarrow 1$  **to**  $N$  **do**

$w_t^i \leftarrow \mathcal{L}(\theta_{t-1}^i)^{\beta_t - \beta_{t-1}};$  /\* Compute unnormalized importance weights \*/

$\mathcal{Z}_t \leftarrow \mathcal{Z}_{t-1} \times N^{-1} \sum_{i=1}^N w_t^i;$  /\* Update marginal likelihood \*/

**for**  $i \leftarrow 1$  **to**  $N$  **do**

$W_t^i \leftarrow w_t^i \times \mathcal{Z}_t / \mathcal{Z}_{t-1};$  /\* Normalize importance weights \*/

$\{\tilde{\theta}_t^i\}_{i=1}^N \sim \text{resample}(\{\theta_{t-1}^i\}_{i=1}^N, \{W_t^i\}_{i=1}^N);$  /\* Resample particles \*/

**for**  $i \leftarrow 1$  **to**  $N$  **do**

$\theta_t^i \leftarrow \mathcal{K}_t(\tilde{\theta}_t^i);$  /\* Propagate particles \*/

---

## 2.2 Computing Posterior Expectation Values

### 2.2.1 Standard Approach

The canonical approach of using the output of SMC to compute expectation values is to use final population of particles. The estimate of a posterior expectation value, that is,

$$\mathbb{E}_{\mathcal{P}}[f] = \int_{\Theta} f(\theta) \mathcal{P}(\theta) d\theta \quad (8)$$

is given by

$$\hat{f} = \frac{1}{N} \sum_{i=1}^N f(\theta_T^i) \quad (9)$$

### 2.2.2 Recycling

When it comes to the estimation of posterior expectation values, the standard approach can be wasteful as it only considers the final positions of the particles,  $\theta_T^i$ , and discards the previous generations of particles,  $\theta_t^i$  for  $t = 1, \dots, T - 1$ , that do not target the posterior directly. To

remedy this uneconomical use of computation, several recycling schemes have been proposed that aim to reweight samples drawn from  $p_t(\theta)$  with  $t \neq T$  to target  $p_T(\theta)$ .

Gramacy et al. (2010) proposed a technique to combine multiple estimates  $\hat{f}_t$  into a single one given by

$$\hat{f} = \sum_{t=1}^T \lambda_t \hat{f}_t \quad (10)$$

where  $\lambda_t = \text{ESS}'_t / \sum_{t=1}^T \text{ESS}'_t$  is the normalized ESS of the particles  $\theta_t^i$  reweighted to target the posterior. The motivation behind this method is that estimators that have low ESS will generally contribute less to the final estimate than those with high ESS. Although originally proposed in the context of importance tempering, Nguyen et al. (2014) and Finke (2015) extended this approach to SMC.

An alternative approach for combining samples drawn from multiple distributions  $p_t(\theta)$  is to assume that the total collection of samples are drawn from the mixture of distributions  $p_t(\theta)$ , where the mixture weights represent the proportion of samples coming from each distribution (Veach and Guibas, 1995; Owen and Zhou, 2000; Elvira et al., 2019). In the case of equal proportions, the importance density is defined as:

$$\tilde{p}(\theta) = \frac{1}{T} \sum_{t=1}^T p_t(\theta) \quad (11)$$

where the densities  $p_t(\theta)$  need to be properly normalized. Using Eq. 11 as the importance density, the importance weights for particles of all iterations are:

$$\tilde{w}_t^i = \frac{\mathcal{L}(\theta_t^i)}{\frac{1}{T} \sum_{t'=1}^T \mathcal{L}(\theta_t^i)^{\beta_{t'}} \mathcal{Z}_t^{-1}} \quad (12)$$

for  $i = 1, \dots, N$  and  $t = 1, \dots, T$ . Since the normalization constants  $\mathcal{Z}_t$  are generally unknown, one could use their SMC estimates given by Eq. 5. Additionally, one could use the weights of Eq. 12 to estimate the normalizing constant  $\mathcal{Z}_T$ . However, as shown elsewhere and further verified in Section 4, this yields only marginally better estimates at the expense of a more complicated estimator (South et al., 2019).

Nguyen et al. (2014) compared the ESS-based recycling approach to the mixture-based one and deduced that the latter performs marginally better despite relying on estimates of the normalizing constant  $\mathcal{Z}_t$ . Our own experiments verified this conclusion and indicated that the noisy estimates of  $\mathcal{Z}_t$  are less problematic than the noisy estimates of the  $\lambda_t$  factors in Eq. 10. In our tests, the latter typically required *ad hoc* thresholds to perform well. For these reasons, we will use the mixture-based approach of recycling in our numerical experiments in Section 4. We will refer to SMC with recycling as *recycled sequential Monte Carlo* (RSMC).

### 3 Method

The computational cost of SMC scales approximately linearly with the number of particles. As the target distribution becomes more complex and high-dimensional, a greater number of particles is required for accurate posterior and evidence approximation. This can render SMC prohibitively expensive for many applications, forcing researchers to either use an insufficient number of particles, leading to potentially biased and high-variance estimates, or resort to alternative sampling methods. Recycling procedures aim to alleviate this issue, but their effectiveness is limited when the number of particles is low. For instance, when using SMC with a low number of particles to sample a high-dimensional multimodal posterior distribution starting from a unimodal prior, mode collapse can occur, where all particles concentrate on a single dominant mode, leading to biased inferences. Recycling would provide a better approximation of the sampled mode but still miss the other modes. This problem can be mitigated by increasing the number of particles or ESS at the cost of higher computational expense.

We argue that the aforementioned inefficiencies of SMC stem from the fact that, at each iteration, SMC represents the current target with a constant-size collection of equally weighted particles. We introduce PS, a general sampling framework for particle-based Bayesian computation that lifts this constraint of SMC. Particularly, in PS, the current target is represented by a growing, weighted collection of particles, termed persistent particles, that are distributed across multiple iterations. PS aims to address the inefficiency of SMC by allowing particles from previous iterations to persist, thus providing a larger and richer pool of particles at no additional computational cost. To achieve this in practice, in every iteration, PS reweights and resamples particles from all previous iterations, not just the last one. Equivalently, this can be thought of as a form continuous recycling that takes place throughout the run. This property of persistence helps PS avoid getting trapped in a single mode and provides a richer approximation of the target posterior distribution, eventually leading to unbiased low-variance posterior and evidence estimates.

#### 3.1 Persistent Sampling

Similar to SMC, PS traverses a sequence of probability distributions,  $p_t(\theta)$  for  $t = 1, \dots, T$ , through a series of reweighting, resampling, and moving steps, as illustrated in Fig. 1. The main difference is that the current collection of particles,  $\{\theta_t^i\}_{i=1}^M$ , at any iteration does not simply originate from the previous distribution,  $p_{t-1}(\theta)$ , by means of the aforementioned three operations. In contrast, particles are reweighted and resampled from all previous iterations, not just the last one. In other words, the particle approximation of  $p_{t-1}(\theta)$  is determined directly by the particle approximations of  $p_s(\theta)$  for  $s = 1, \dots, t-1$ . The PS pseudocode is presented in detail in Algorithm 2.

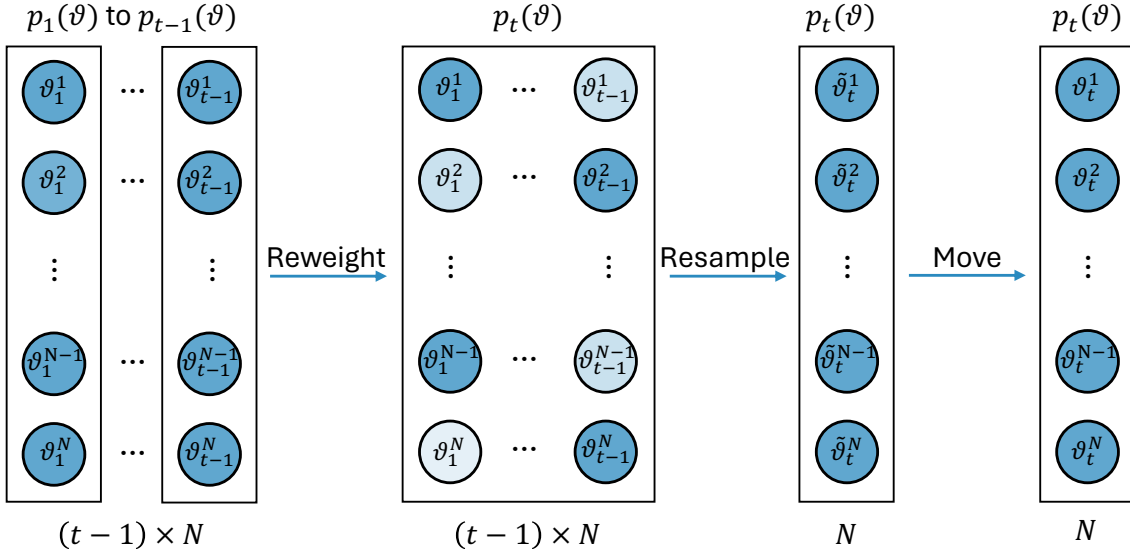


Figure 1: Illustration of the reweighting, resampling, and moving steps in PS. The  $(t-1) \times N$  particles representing  $p_1(\theta)$  to  $p_{t-1}(\theta)$  are reweighted to target  $p_t(\theta)$ . Out of these  $(t-1) \times N$  particles,  $N$  are resampled and moved to better approximate  $p_t(\theta)$ .

### 3.1.1 Reweighting

In the reweighting step, PS assigns a single weight  $W_{tt'}^i$  to each particle  $\theta_{t'}^i$ , where  $t$  and  $t' < t$  denote the current and past iteration, respectively. The aim is that the weighted particles will target  $p_t(\theta)$  despite being drawn from different distributions. Similar to multiple importance sampling (Veach and Guibas, 1995; Veach, 1998), we can treat  $\theta_{t'}^i$  for  $t' = 1, \dots, t-1$  and  $i = 1, \dots, N$  as samples from the mixture distribution

$$\tilde{p}_t(\theta) = \frac{1}{t-1} \sum_{s=1}^{t-1} p_s(\theta), \quad (13)$$

where  $p_s(\theta)$  is the usual annealed target at iteration  $s$ . Employing Eq. 13 as the importance density, we can derive the following weights:

$$W_{tt'}^i = \frac{p_t(\theta_{t'}^i)}{\frac{1}{t-1} \sum_{s=1}^{t-1} p_s(\theta_{t'}^i)} = \frac{w_{tt'}^i}{\mathcal{Z}_t}, \quad (14)$$

where the  $w_{tt'}^i$  are the unnormalized weights given by

$$w_{tt'}^i = \frac{\mathcal{L}(\theta_{t'}^i)^{\beta_t}}{\frac{1}{t-1} \sum_{s=1}^{t-1} \mathcal{L}(\theta_{t'}^i)^{\beta_s} \mathcal{Z}_s^{-1}} \quad (15)$$

for  $t' = 1, \dots, t-1$  and  $i = 1, \dots, N$ . The normalization constant  $\mathcal{Z}_t$  can be estimated as

$$\mathcal{Z}_t = \frac{1}{t-1} \sum_{t'=1}^{t-1} \left( \frac{1}{N} \sum_{i=1}^N w_{tt'}^i \right) \quad (16)$$

However, unlike SMC, the ESS in PS is computed using the persistent weights. Since the persistent particles are generally more numerous than the standard particles of SMC, the ESS in PS can, in principle, be many times greater than in SMC. The ESS of the persistent particles is defined as:

$$\text{ESS}_t = \frac{\left[ \sum_{t'=1}^{t-1} \left( \sum_{i=1}^N w_{tt'}^i \right) \right]^2}{\sum_{t'=1}^{t-1} \left[ \sum_{i=1}^N (w_{tt'}^i)^2 \right]} = \frac{1}{\sum_{t'=1}^{t-1} \left[ \sum_{i=1}^N (W_{tt'}^i)^2 \right]} \quad (17)$$

PS determines the next temperature level,  $\beta_t$ , adaptively by maintaining a constant ESS throughout the run, similarly to SMC. To find the next  $\beta_t$ , one needs to solve Eq. 7 numerically. However,  $\alpha$  is no longer restricted to be strictly smaller than 1, and can take values in the interval  $(0, t-1)$ . When  $\alpha \geq 1$ , in the initial  $\lfloor \alpha \rfloor + 1$  iterations of PS,  $\beta_t$  will repeatedly be set to 0 and  $p_t(\theta)$  will remain the prior distribution  $\pi(\theta)$ . This provides the option to reduce the computational cost of these initial iterations by performing independent sampling from the prior instead of MCMC transitions. After iteration  $\lfloor \alpha \rfloor + 1$ , the value of  $\beta$  will start increasing as usual, annealing the distribution from the prior toward the posterior.

PS typically terminates when  $\beta_t$  becomes 1, corresponding to the target posterior distribution. However, an additional advantage of PS is that one can continue sampling even after  $\beta_t = 1$  until a prespecified ESS is gathered. In this scenario,  $\beta_t = \beta_{t+1} = \dots = \beta_{T-1} = \beta_T = 1$ . This can provide more samples from the posterior distribution without going through all the  $T$  iterations from the beginning.

### 3.1.2 Resampling

Resampling of particles in PS can be performed using the same techniques as in SMC (i.e., multinomial resampling, systematic resampling, etc.). However, the difference is that in PS one generally resamples  $N$  new particles from  $(t-1) \times N \geq N$  persistent particles. In other words, the pool of available candidates grows throughout the run but the number of resampled particles remains the same. This is, at least partially, the reason for the improved performance of PS compared to SMC. *Propagation of chaos* theory suggests that in the limit where  $N \ll (t-1) \times N$ , the  $N$  resampled particles behave essentially as independent samples from the probability distribution (Moral, 2004). This means that the  $N$  resampled particles in PS are less correlated than the respective  $N$  resampled particles in SMC.

### 3.1.3 Moving

Unlike the reweighting and resampling steps of PS that constitute clear extensions of the respective SMC components, the moving step is largely unaltered. In other words, the same MCMC methods can be used to diversify the particles following the resampling steps. That said, the moving step in PS boasts a major advantage – the adaptation of the MCMC kernel can be performed by utilizing the more numerous persistent particles. This naturally leads to kernels that

better adapt to the geometrical characteristics of the target. For instance, in the case where a covariance matrix needs to be adapted, typically at least  $N \geq 2 \times D$  particles are required to get a non-singular estimate. In high-dimensions this can become prohibitively expensive for standard SMC. In contrast, the same covariance matrix estimation in PS is performed utilizing  $(t - 1) \times N \geq N$  samples. Furthermore, even in cases where the number of SMC particles are sufficient, PS will still lead to better estimates given the greater size of its ensemble of persistent particles. The same principles apply to the estimation of components of more complicated kernels (e.g., mixture distributions, normalizing flows, etc.).

---

**Algorithm 2:** Persistent Sampling

---

**Data:** Number of particles  $N$ , ESS fraction  $\alpha$ , prior density  $\pi(\theta)$ , likelihood function  $\mathcal{L}(\theta)$ , Markov kernel  $\mathcal{K}_t$  with invariant density  $p_t(\theta)$

**Result:** Samples  $\{\theta_T^i\}_{i=1}^N$  from  $\mathcal{P}(\theta) = \mathcal{L}(\theta)\pi(\theta)/\mathcal{Z}$  and marginal likelihood estimate  $\mathcal{Z} \equiv \mathcal{Z}_T$

$t \leftarrow 1, \beta_t \leftarrow 0, \mathcal{Z}_1 \leftarrow 1;$

**for**  $i \leftarrow 1$  **to**  $N$  **do**

$\theta_1^i \sim \pi(\theta);$  /\* Sample prior distribution \*/

**while**  $\beta_t < 1$  **do**

$t \leftarrow t + 1;$

$\beta_t \leftarrow \inf_{\beta \in [\beta_{t-1}, 1]} \{\text{ESS}_t \geq \alpha N\};$  /\* Update temperature \*/

**for**  $t' \leftarrow 1$  **to**  $t$  **do**

**for**  $i \leftarrow 1$  **to**  $N$  **do**

$w_{tt'}^i \leftarrow \frac{\mathcal{L}(\theta_{t'}^i)^{\beta_t}}{\frac{1}{t-1} \sum_{s=1}^{t-1} \mathcal{L}(\theta_{t'}^i)^{\beta_s} \mathcal{Z}_s^{-1}};$  /\* Compute unnormalized importance weights \*/

$\mathcal{Z}_t \leftarrow \frac{1}{t-1} \sum_{t'=1}^{t-1} \left( \frac{1}{N} \sum_{i=1}^N w_{tt'}^i \right);$  /\* Update marginal likelihood \*/

**for**  $t' \leftarrow 1$  **to**  $t$  **do**

**for**  $i \leftarrow 1$  **to**  $N$  **do**

$W_{tt'}^i \leftarrow \frac{w_{tt'}^i}{\mathcal{Z}_t};$  /\* Normalize importance weights \*/

$\{\tilde{\theta}_t^i\}_{i=1}^N \sim \text{resample}(\{\{\theta_{t'}^i\}_{i=1}^N\}_{t'=1}^{t-1}, \{\{W_{tt'}^i\}_{i=1}^N\}_{t'=1}^{t-1});$  /\* Resample particles \*/

**for**  $i \leftarrow 1$  **to**  $N$  **do**

$\theta_t^i \leftarrow \mathcal{K}_t(\tilde{\theta}_t^i);$  /\* Propagate particles \*/

---

### 3.2 Computing Expectations

Computing posterior expectation values in PS can be done by utilizing the persistent particles with their associated normalized weights. This leads to estimators of the form:

$$\hat{f} = \frac{1}{T} \sum_{t'=1}^T \left[ \frac{1}{N} \sum_{i=1}^N W_{Tt'}^i f(\theta_{t'}^i) \right] \quad (18)$$

where  $T$  is the total number of iterations. Of course one could alternatively resample the persistent particles  $\theta_{t'}^i$  with weights  $W_{Tt'}^i$  at the end of the run and use the resampled particles  $\tilde{\theta}_T^i$  to compute expectations. However, the use of the weighted persistent particles should be preferred when possible since the resampling procedure can introduce some variance.

### 3.3 Practical Considerations

In PS, there is a computational trade-off between increasing the number of particles,  $N$ , and the ESS fraction,  $\alpha$  (even to values above 1). As we will see in Section 4, for estimating posterior expectations, it does not significantly matter which parameter is increased, as both approaches lead to a richer ensemble of persistent particles and hence more accurate estimates. However, for the estimation of marginal likelihoods, increasing  $N$  seems to give substantially superior results and should therefore be preferred over increasing  $\alpha$  alone. Increasing  $N$  offers another practical advantage: it allows for better utilization of parallel computing resources, if available. Since the computations for each particle are independent during the “moving” step, a larger  $N$  enables more effective parallelization, leading to additional computational savings.

## 4 Experiments

The primary computational burden of SMC methods stems from the large number of particles required to obtain accurate estimates of the posterior distribution and marginal likelihood/model evidence. To demonstrate that our proposed PS approach can achieve a substantially higher sampling efficiency, while keeping all other factors equal (e.g., total computational cost in likelihood evaluations, number of MCMC steps per iteration, choice of MCMC kernel, effective sample size percentage threshold), we designed a comprehensive suite of numerical experiments (i.e., Gaussian mixture, Rosenbrock, sparse logistic regression, and Bayesian hierarchical model). The comparison was performed among SMC, RSMC (i.e., SMC with recycling), and PS.

To assess the accuracy of the posterior approximation, we estimate the maximum squared bias across dimensions, defined as:

$$b_i^2 = \max_d \left( \frac{\hat{f}_i - \mu(f_i)}{\sigma(f_i)} \right)^2 \quad (19)$$

for the first and second posteriors moments,  $f_1 = \theta$  and  $f_2 = \theta^2$ , respectively (Hoffman and Sountsov, 2022). To estimate  $\hat{f}_i$ , we computed the average  $f_i$  across 100 independent runs of each algorithm. To estimate the posterior mean,  $\mu(f_i)$ , and posterior standard deviation,  $\sigma(f_i)$ , we used 100 extended runs of standard SMC with 16,384 particles and an extremely conservative effective sample size threshold ( $\alpha = 0.999$ ). To quantify the variance and bias of the log model evidence estimates,  $\log \mathcal{Z}$ , we simply computed their mean squared error (MSE) given that they are scalar quantities. The ground truth for this estimate was computed using the aforementioned 100 extended SMC runs. Finally, to account for the computational cost, we define the sampling efficiency as the reciprocal of the product of a metric (i.e.,  $b_1^2$ ,  $b_1^2$ , or  $\text{MSE}_{\log \mathcal{Z}}$ ) with the total number of likelihood calls.

All methods utilized 250 RWM steps per iteration in their moving step. This uniform approach was key in creating a fair basis for comparing PS and SMC. We had a couple of main reasons for this choice. Firstly, we wanted to control as many variables as possible, aside from the method itself. This was crucial to ensure that any observed differences were genuinely due to the method and not influenced by other factors. Secondly, opting for a larger number of steps was a deliberate strategy. It gave the particles ample time to achieve equilibrium in each iteration, which is vital. Proper equilibration means that the particles more accurately represent the current target distribution  $p_t(\theta)$ , approximating independent samples from it. The proposal covariance matrix was estimated from the initial particle distribution and was rescaled to achieve an acceptance rate of 0.234.

#### 4.1 Gaussian Mixture

A challenging benchmark problem for evaluating the performance of SMC algorithms is sampling from a multimodal distribution with well-separated modes. We consider a 16-dimensional bimodal double *Gaussian mixture* model with a likelihood function:

$$\mathcal{L}(\boldsymbol{\theta}) = \frac{1}{3}\mathcal{N}(\boldsymbol{\theta}|-5, \mathbf{I}) + \frac{2}{3}\mathcal{N}(\boldsymbol{\theta}|5, \mathbf{I}) \quad (20)$$

with a multivariate uniform distribution  $\pi(\boldsymbol{\theta}) = \mathcal{U}(\boldsymbol{\theta}|-10, 10)$  as the prior. This bimodal target features well-separated and unequally weighted modes, making it difficult for samplers to efficiently explore the two modes and accurately estimate properties like the normalizing constant and the relative weight of the two modes. Fig. 2 shows the 1D and 2D marginal posterior contours for the first three parameters of this target sampled using PS (blue) with  $N = 1024$  and  $\alpha = 0.99$ , as well as the reference SMC configuration (grey), exhibiting good agreement. The figure also demonstrates that no mode collapse has occurred in this case and both posterior peaks are correctly represented.

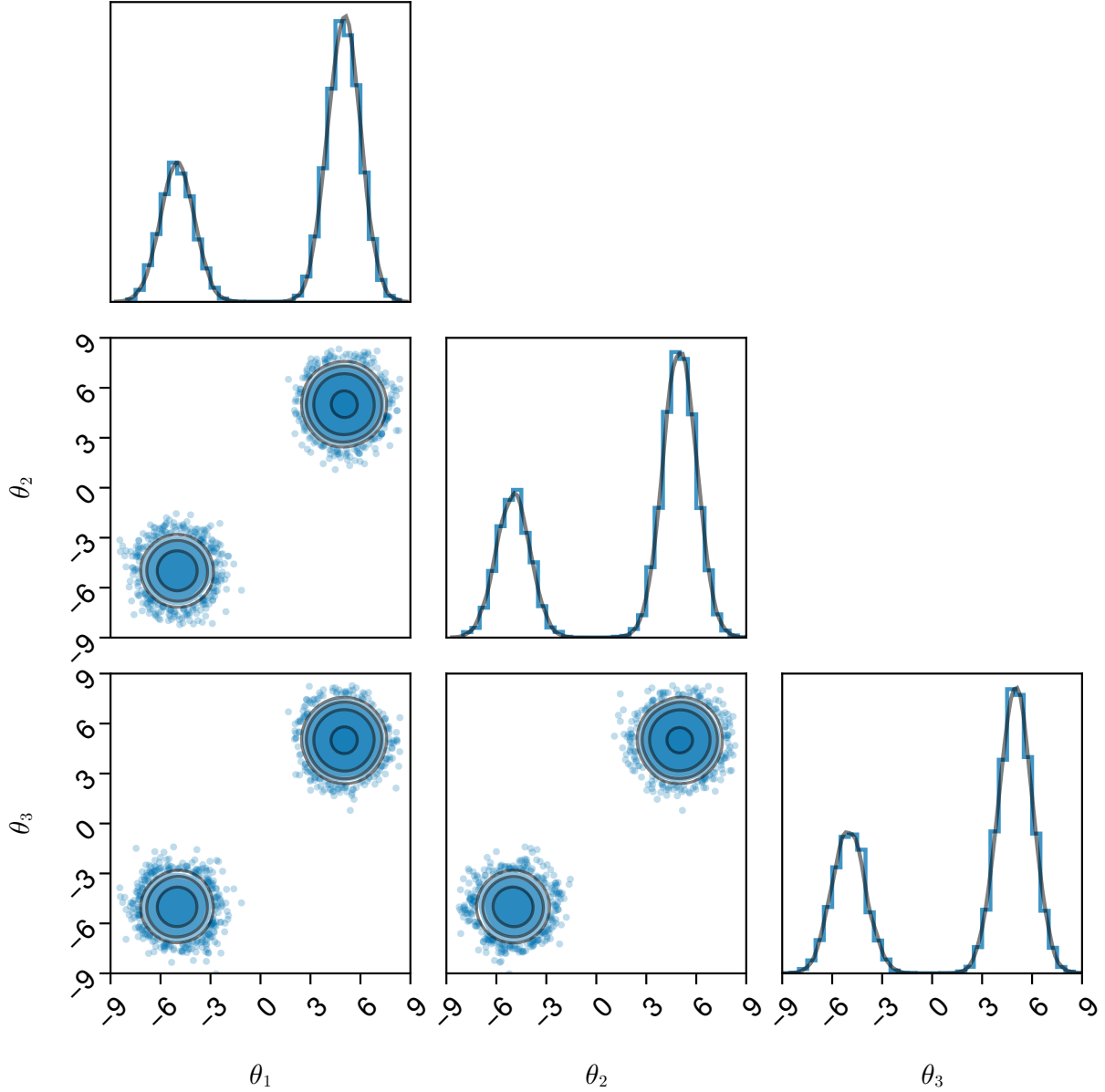


Figure 2: 1D and 2D marginal posterior distributions of the first three parameters of the Gaussian mixture target. Blue contours indicate the output of PS and black that of a very long SMC run considered as the reference truth.

The Gaussian mixture benchmark highlights PS’s effectiveness in handling multimodal posterior distributions. Table 1 shows PS achieves significantly lower squared bias,  $b_i^2$  for  $i = 1, 2$ , in estimating the first two posterior moments and more accurate marginal likelihood estimates (lower  $\text{MSE}_{\log \mathcal{Z}}$ ) compared to SMC, with and without recycling, with the same computational budget. These improvements stem from PS’s ability to maintain a larger, more diverse set of particles, preventing mode collapse and ensuring comprehensive posterior exploration. Increasing  $\alpha$  in PS reduces  $b_i^2$  but doesn’t significantly improve  $\text{MSE}_{\log \mathcal{Z}}$ , while increasing  $N$  substantially

reduces both. This indicates that increasing  $N$  is preferable when possible. Fig. 3 illustrates the superior sampling efficiency of PS over SMC and RSMC for estimating posterior moments and log marginal likelihood. PS consistently outperforms SMC across all particle counts and ESS fractions  $\alpha$ . Increasing particles in PS yields more substantial gains compared to raising the ESS fraction alone. Recycling (i.e., RSMC) brings marginal improvements, most notably for  $b_2^2$ .

Table 1: Performance comparison of SMC and PS methods for Gaussian mixture target. The computational cost in terms of the number of likelihood evaluations (calls), the squared bias for the first two posterior moments, and the mean square error (MSE) for the logarithm of the marginal likelihood are presented for varying particle numbers and effective sample size (ESS) fractions ( $\alpha$ ). The values in parentheses denote estimates computed using recycling.

Method	N	$\alpha$	Calls ( $\times 10^6$ )	$b_1^2$	$b_2^2$	$MSE_{\log \mathcal{Z}}$
(R)SMC	32	0.90	0.26	0.9627 (0.8851)	0.3094 (0.3062)	24.66 (24.51)
(R)SMC	64	0.90	0.58	0.4370 (0.3668)	0.0260 (0.0068)	2.01 (1.98)
(R)SMC	128	0.90	1.20	0.2249 (0.1780)	0.0118 (0.0032)	0.37 (0.35)
(R)SMC	32	0.99	0.89	1.0645 (1.0258)	0.1297 (0.0748)	19.41 (19.21)
(R)SMC	64	0.99	1.93	0.7279 (0.6744)	0.0240 (0.0027)	1.75 (1.67)
(R)SMC	128	0.99	3.96	0.5491 (0.4595)	0.0123 (0.0012)	0.35 (0.33)
PS	32	0.90	0.08	0.2557	0.0362	3.16
PS	64	0.90	0.18	0.1335	0.0127	1.03
PS	128	0.90	0.38	0.0947	0.0051	0.34
PS	256	0.90	0.81	0.0591	0.0026	0.08
PS	512	0.90	1.64	0.0217	0.0014	0.03
PS	32	0.99	0.09	0.2591	0.0334	3.28
PS	64	0.99	0.19	0.1772	0.0132	1.28
PS	128	0.99	0.41	0.0692	0.0050	0.35
PS	256	0.99	0.87	0.0496	0.0020	0.07
PS	512	0.99	1.76	0.0179	0.0014	0.03
PS	32	2.00	0.13	0.1612	0.0225	3.59
PS	64	2.00	0.30	0.0887	0.0106	1.01
PS	128	2.00	0.64	0.0536	0.0033	0.17
PS	256	2.00	1.35	0.0290	0.0017	0.04

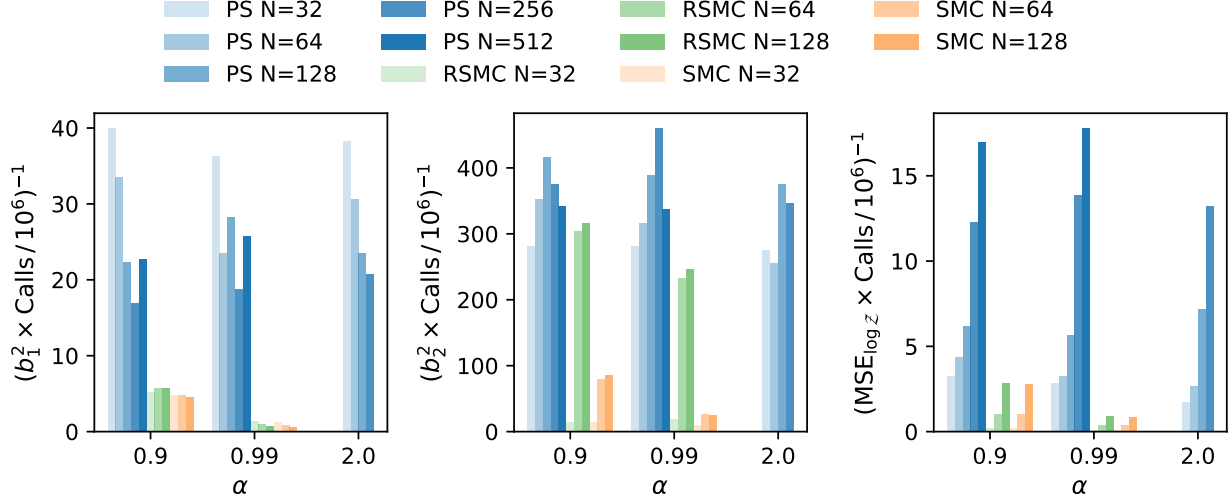


Figure 3: Sampling efficiency for the first (*left*) and second (*middle*) posterior moments (with recycling for SMC) and log model evidence (*right*) for the Gaussian mixture target. Efficiency is quantified as the reciprocal of the product of the metric (e.g.,  $b_1^2$ ,  $b_2^2$ , or  $\text{MSE}_{\log z}$ ) and the number of likelihood evaluations (Calls). Higher values of efficiency indicate better performance. Configurations of SMC and PS are grouped based on their effective sample size (ESS) fraction ( $\alpha$ ) and represented by varying colors according to the number of particles ( $N$ ).

## 4.2 Rosenbrock Function

The *Rosenbrock function* is a well known non-convex optimization benchmark (Rosenbrock, 1960). The function is particularly challenging for optimization algorithms due to its narrow, curved valley containing the minimum. Here we consider a 16-dimensional extension of this function as the log-likelihood function given by

$$\log \mathcal{L}(\boldsymbol{\theta}) = - \sum_{i=1}^8 [10(\theta_{2i-1}^2 - \theta_{2i})^2 + (\theta_{2i-1} - 1)^2] \quad (21)$$

with a multivariate normal distribution  $\pi(\boldsymbol{\theta}) = \mathcal{N}(\boldsymbol{\theta} | 0, 5^2 \mathbf{I})$  as the prior distribution. Fig. 4 shows the 1D and 2D marginal posterior contours for the first three parameters of this target sampled using PS (blue) with  $N = 1024$  and  $\alpha = 0.99$ , as well as and the reference SMC configuration (grey), exhibiting good agreement. The figure demonstrates the non-Gaussian geometry of the posterior distribution that renders this benchmark so challenging.

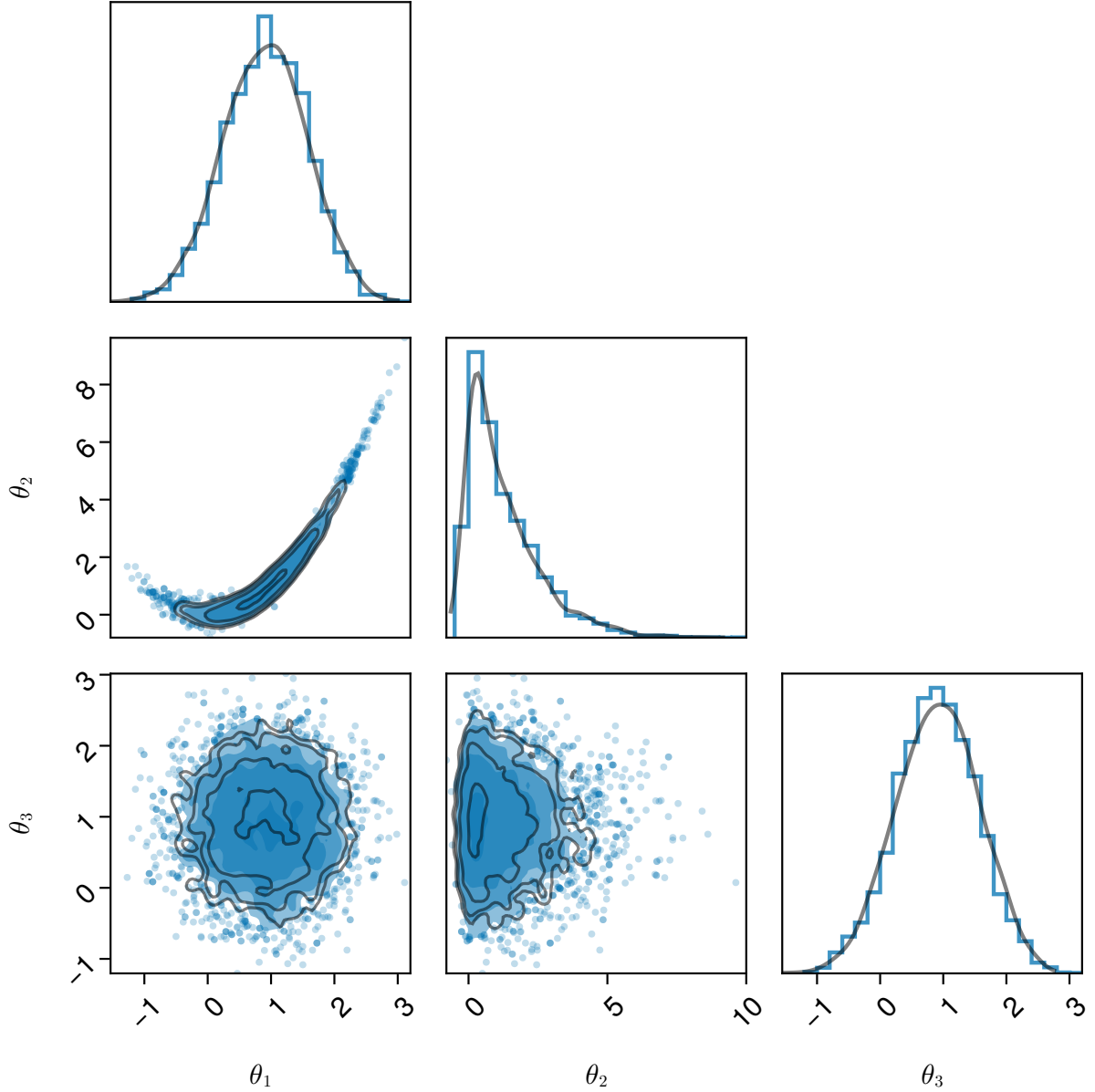


Figure 4: 1D and 2D marginal posterior distributions of the first three parameters of the Rosenbrock target. Blue contours indicate the output of PS and black that of a very long SMC run considered as the reference truth.

The Rosenbrock function experiment showcases PS’s advantages in handling non-convex and high-dimensional target distributions. Table 2 demonstrates PS consistently outperforming SMC in terms of  $b_i^2$  and  $\text{MSE}_{\log \mathcal{Z}}$  across various particle counts and effective sample size thresholds. PS’s persistent particle strategy enables more efficient parameter space exploration, evident in its superior bias reduction and characterization of complex posterior geometry. Consistent with the Gaussian mixture results, increasing  $\alpha$  has limited impact on  $\text{MSE}_{\log \mathcal{Z}}$  compared to increasing  $N$ . Recycling shows marginal improvement in  $\text{MSE}_{\log \mathcal{Z}}$  for SMC. Fig. 5 illustrates PS’s higher

sampling efficiency compared to SMC across all configurations, both for posterior moment estimation and log evidence approximation. Recycling (RSMC) does not significantly enhance  $b_1^2$ ,  $b_2^2$ , or  $\text{MSE}_{\log \mathcal{Z}}$  in this case.

Table 2: Performance comparison of SMC and PS methods for the Rosenbrock target. The computational cost in terms of the number of likelihood evaluations (calls), the squared bias for the first two posterior moments, and the mean square error (MSE) for the logarithm of the marginal likelihood are presented for varying particle numbers and effective sample size (ESS) fractions ( $\alpha$ ). The values in parentheses denote estimates computed using recycling.

Method	N	$\alpha$	Calls ( $\times 10^6$ )	$b_1^2$	$b_2^2$	$\text{MSE}_{\log \mathcal{Z}}$
(R)SMC	32	0.90	0.38	0.3798 (0.3883)	0.2931 (0.2889)	28.63 (28.31)
(R)SMC	64	0.90	0.84	0.0412 (0.0394)	0.0407 (0.0386)	5.92 (5.83)
(R)SMC	128	0.90	1.72	0.0179 (0.0122)	0.0185 (0.0139)	1.38 (1.35)
(R)SMC	32	0.99	1.28	0.1884 (0.1637)	0.1428 (0.1266)	42.24 (41.45)
(R)SMC	64	0.99	2.82	0.0324 (0.0165)	0.0322 (0.0214)	8.96 (8.69)
(R)SMC	128	0.99	5.81	0.0177 (0.0066)	0.0180 (0.0091)	2.63 (2.52)
PS	32	0.90	0.13	0.7471	0.5846	30.48
PS	64	0.90	0.31	0.2357	0.1700	9.06
PS	128	0.90	0.66	0.0520	0.0390	2.64
PS	256	0.90	1.37	0.0104	0.0104	0.26
PS	512	0.90	2.81	0.0039	0.0042	0.09
PS	32	0.99	0.14	0.7219	0.5762	29.53
PS	64	0.99	0.33	0.2293	0.1809	9.36
PS	128	0.99	0.71	0.0448	0.0293	2.67
PS	256	0.99	1.47	0.0104	0.0104	0.25
PS	512	0.99	3.04	0.0038	0.0039	0.06
PS	32	2.00	0.24	0.4287	0.4402	26.95
PS	64	2.00	0.55	0.1288	0.1340	7.53
PS	128	2.00	1.18	0.0272	0.0226	2.16
PS	256	2.00	2.42	0.0056	0.0061	0.22

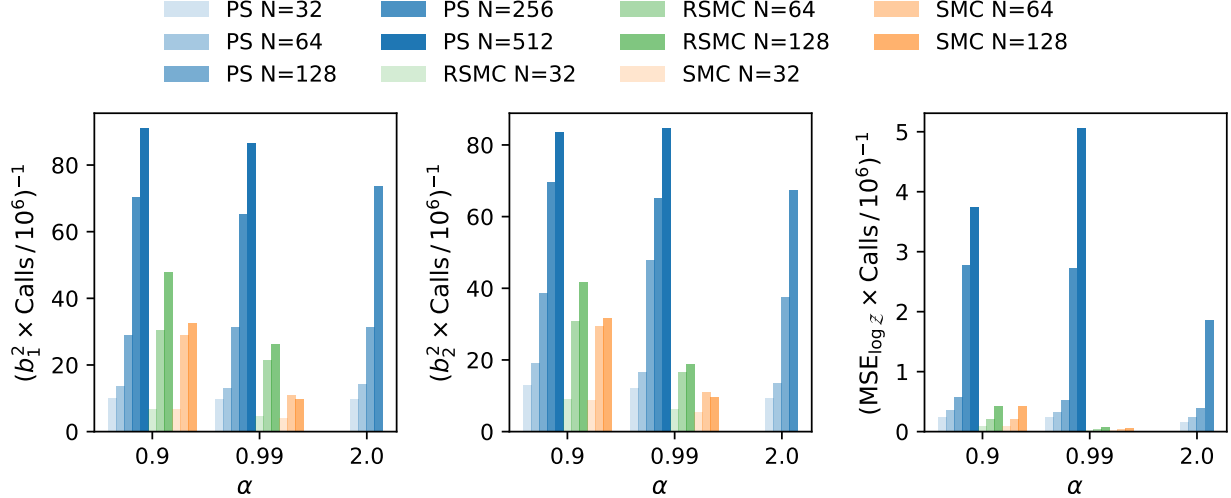


Figure 5: Sampling efficiency for the first (*left*) and second (*middle*) posterior moments (with recycling for SMC) and log model evidence (*right*) for the Rosenbrock target. Efficiency is quantified as the reciprocal of the product of the metric (e.g.,  $b_1^2$ ,  $b_2^2$ , or  $MSE_{\log z}$ ) and the number of likelihood evaluations (Calls). Higher values of efficiency indicate better performance. Configurations of SMC and PS are grouped based on their effective sample size (ESS) fraction ( $\alpha$ ) and represented by varying colors according to the number of particles ( $N$ ).

### 4.3 Sparse Logistic Regression

In this experiment, we explore a *sparse logistic regression* model in 51 dimensions, applied to the German credit dataset (Dua and Graff, 2017). This dataset comprises 1,000 data points, each representing an individual who has borrowed from a financial institution. The dataset classifies these individuals into two categories: those deemed as good credit risks and those considered bad credit risks, according to the bank’s evaluation criteria. Each data point contains 24 numerical covariates, which may or may not serve as useful predictors for determining credit risk. These covariates include factors such as age, gender, and savings information. The model incorporates a hierarchical structure and utilizes a horseshoe prior for the logistic regression parameters (Carvalho et al., 2009). The horseshoe prior promotes sparsity in the regression coefficients, effectively performing variable selection.

We define the likelihood function as follows:

$$\mathcal{L}(\mathbf{y}|\boldsymbol{\beta}, \boldsymbol{\lambda}, \tau) = \prod_{i=1}^{1000} \text{Bernoulli} \left( y_i | \sigma((\tau \boldsymbol{\lambda} \odot \boldsymbol{\beta})^T \mathbf{X}_i) \right), \quad (22)$$

where  $\sigma(\cdot)$  denotes the sigmoid function.  $\boldsymbol{\beta}$  and  $\boldsymbol{\lambda}$  are 25-dimensional vectors and  $\tau$  is a scalar quantity. The priors for the model parameters are given by:

$$\pi(\boldsymbol{\beta}, \boldsymbol{\lambda}, \tau) = \text{Gamma}(\tau|1/2, 1/2) \prod_{j=1}^{25} \mathcal{N}(\beta_j|0, 1) \text{Gamma}(\lambda_j|1/2, 1/2). \quad (23)$$

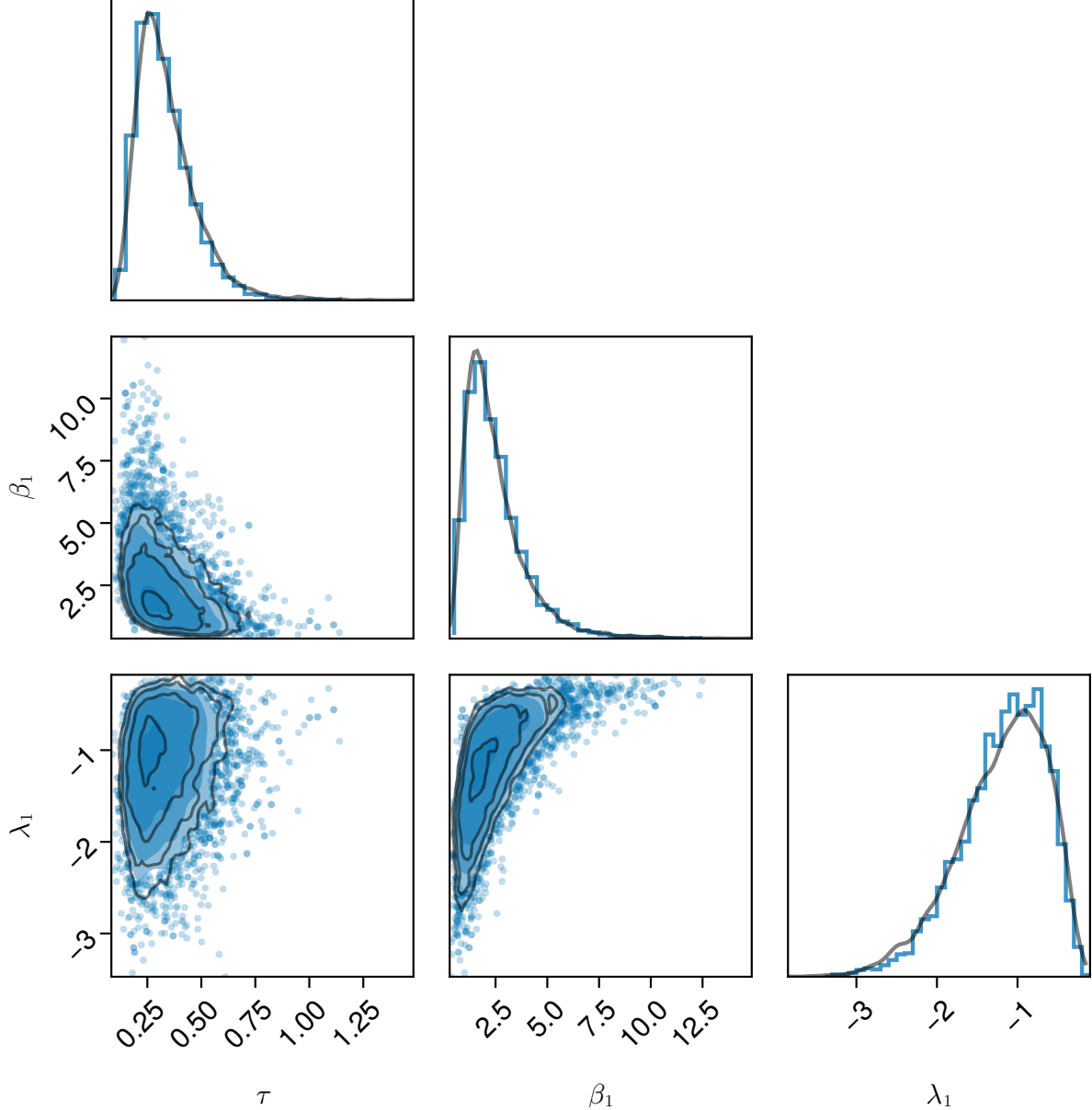


Figure 6: 1D and 2D marginal posterior distributions of the  $\tau$ ,  $\beta_1$ , and  $\lambda_1$  parameters of the sparse logistic regression with the German credit data. Blue contours indicate the output of PS and black that of a very long SMC run considered as the reference truth.

Fig. 6 shows the 1D and 2D marginal posterior contours for the  $\tau$ ,  $\beta_1$ , and  $\lambda_1$  parameters of this target sampled using PS (blue) with  $N = 1024$  and  $\alpha = 0.99$ , as well as and the reference SMC configuration (grey), exhibiting good agreement. The figure also demonstrates the highly non-Gaussian nature of this target originating by the hierarchical structure of the model.

Table 3: Performance comparison of SMC and PS methods for the sparse logistic regression with the German credit data. The computational cost in terms of the number of likelihood evaluations (calls), the squared bias for the first two posterior moments, and the mean square error (MSE) for the logarithm of the marginal likelihood are presented for varying particle numbers and effective sample size (ESS) fractions ( $\alpha$ ). The values in parentheses denote estimates computed using recycling.

Method	N	$\alpha$	Calls ( $\times 10^6$ )	$b_1^2$	$b_2^2$	$MSE_{\log \mathcal{Z}}$
(R)SMC	128	0.90	1.10	0.0549 (0.0467)	0.0739 (0.0712)	25.84 (25.62)
(R)SMC	256	0.90	2.35	0.0186 (0.0136)	0.0255 (0.0207)	5.50 (5.44)
(R)SMC	512	0.90	4.85	0.0068 (0.0056)	0.0089 (0.0074)	1.17 (1.16)
(R)SMC	128	0.99	3.54	0.0495 (0.0388)	0.0659 (0.0606)	46.54 (45.41)
(R)SMC	256	0.99	7.67	0.0170 (0.0100)	0.0235 (0.0168)	10.92 (10.57)
PS	128	0.90	0.50	0.0434	0.0494	3.31
PS	256	0.90	1.05	0.0207	0.0196	0.87
PS	512	0.90	2.17	0.0094	0.0095	0.33
PS	1024	0.90	4.42	0.0069	0.0063	0.13
PS	2048	0.90	9.10	0.0038	0.0036	0.03
PS	128	0.99	0.53	0.0350	0.0543	2.77
PS	256	0.99	1.11	0.0219	0.0201	0.91
PS	512	0.99	2.31	0.0096	0.0097	0.28
PS	1024	0.99	4.72	0.0059	0.0058	0.10
PS	2048	0.99	9.72	0.0032	0.0036	0.03
PS	128	2.00	0.82	0.0263	0.0234	2.97
PS	256	2.00	1.75	0.0162	0.0171	0.97
PS	512	2.00	3.64	0.0064	0.0062	0.28
PS	1024	2.00	7.44	0.0044	0.0049	0.08

In the sparse logistic regression benchmark with German credit data, PS outperforms SMC as shown in Table 3. PS achieves lower  $b_i^2$  and  $MSE_{\log \mathcal{Z}}$  with a smaller computational budget, due to its ability to maintain diverse, informative persistent particles. This is crucial for capturing the sparsity-inducing horseshoe prior and identifying relevant predictors in high-dimensional covariate space. Consistent with previous findings, increasing  $\alpha$  primarily benefits posterior moment estimates, while increasing N improves both posterior and marginal likelihood accuracy. Recycling does not significantly enhance log marginal likelihood estimate accuracy for SMC in this problem. Fig. 7 demonstrates PS's superior sampling efficiency compared to SMC across various particle counts and effective sample sizes. As before, recycling (RSMC) brings only marginal

improvements in  $b_1^2$ ,  $b_2^2$ , and  $\text{MSE}_{\log \mathcal{Z}}$ .

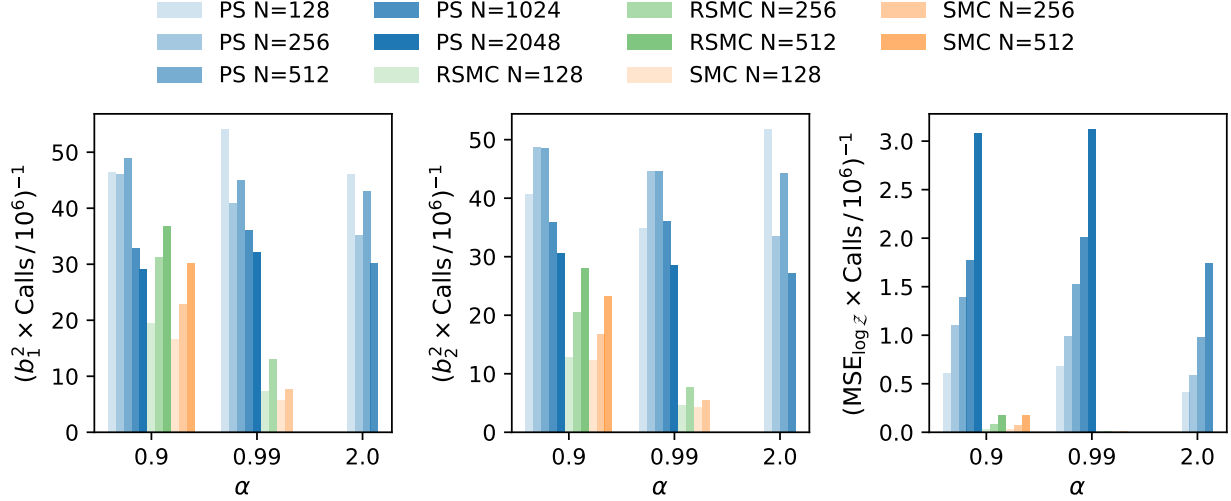


Figure 7: Sampling efficiency for the first (*left*) and second (*middle*) posterior moments (with recycling for SMC) and log model evidence (*right*) for the sparse logistic regression target with German credit data. Efficiency is quantified as the reciprocal of the product of the metric (e.g.,  $b_1^2$ ,  $b_2^2$ , or  $\text{MSE}_{\log \mathcal{Z}}$ ) and the number of likelihood evaluations (Calls). Higher values of efficiency indicate better performance. Configurations of SMC and PS are grouped based on their effective sample size (ESS) fraction ( $\alpha$ ) and represented by varying colors according to the number of particles ( $N$ ).

#### 4.4 Bayesian Hierarchical Model

*Bayesian hierarchical modeling* (BHM) plays a critical role in contemporary science, integrating multiple sub-models within a unified framework (Gelman et al., 1995). In this approach, a global parameter set,  $\theta$ , influences the individual, local parameters  $z$ , which in turn model the observed data  $D$ . The relationship among these elements is encapsulated in the posterior distribution:

$$p(\theta, z|D) \propto p(D|z)p(z|\theta)p(\theta), \quad (24)$$

with the data's likelihood function dependent solely on local parameters. A notable aspect of BHM is the funnel-like structure of its posterior distribution. This complex geometry can challenge the efficiency of MCMC sampling methods, although certain reparameterizations can mitigate these difficulties (Papaspiliopoulos et al., 2007).

Following the concept of Neal's funnel (Neal, 2003), our model sets the global parameter distribution as  $p(\theta) = \mathcal{N}(\theta|0, \tau^2)$  and the local parameter conditional distribution as  $p(z|\theta) = \mathcal{N}(z|0, \exp(\theta)\mathbf{I})$ . We assume a normal sampling distribution for the data  $p(\mathbf{D}|z) = \mathcal{N}(\mathbf{D}|z, \sigma^2\mathbf{I})$ . The data for our experiment were generated under the condition  $\theta = -2$  with  $\tau = 2$  and  $\sigma = 1$ . The model considers  $\theta$  as a scalar, while  $z$  and  $\mathbf{D}$  are 30-dimensional vectors, resulting in a total

of 31 parameters in the model. Fig. 8 shows the 1D and 2D marginal posterior contours for the first three parameters of this target sampled using PS (blue) with  $N = 1024$  and  $\alpha = 0.99$ , as well as and the reference SMC configuration (grey), exhibiting good agreement. The funnel structure is clear in the  $\theta-z_i$  marginal posterior contours.

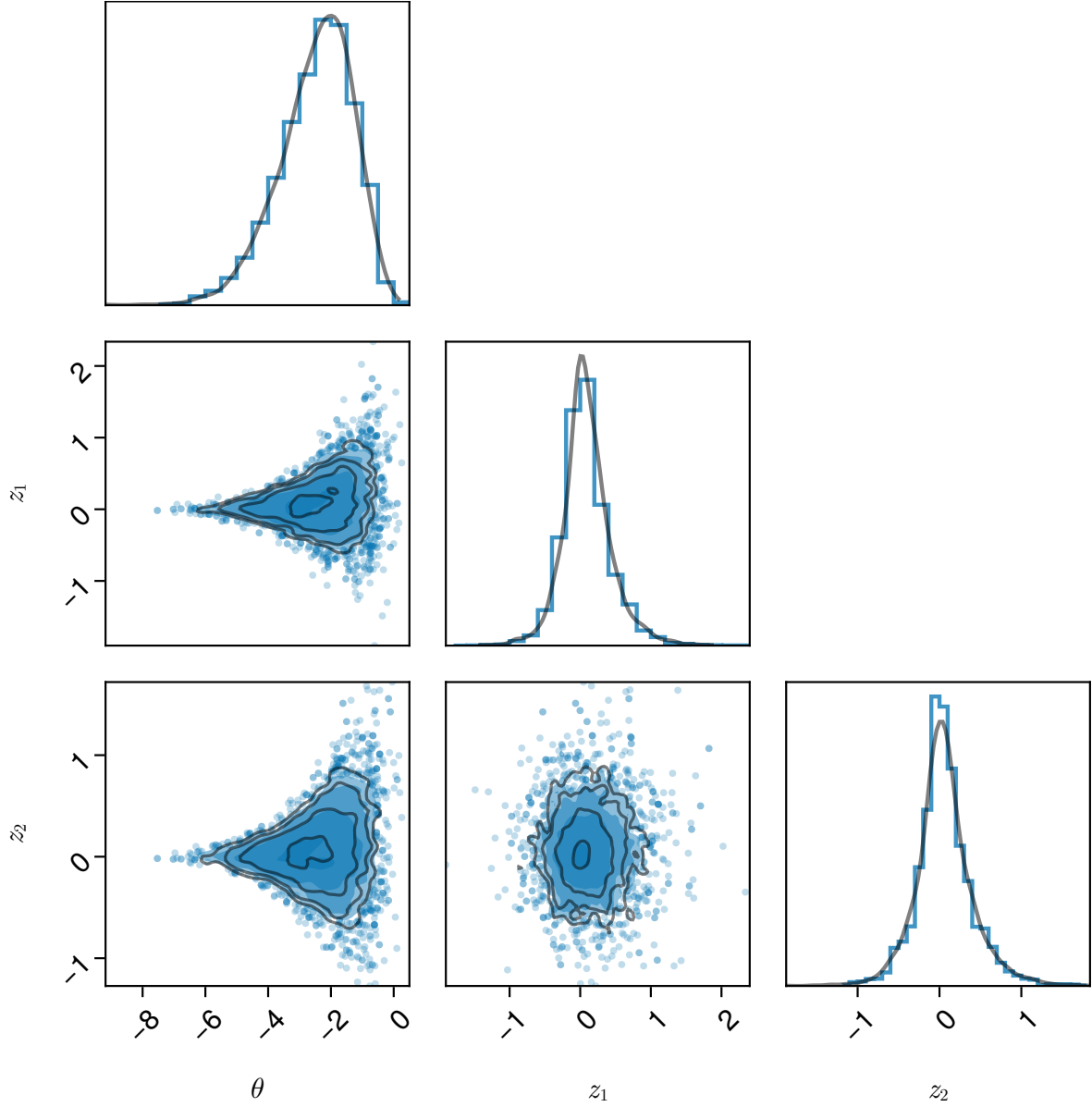


Figure 8: 1D and 2D marginal posterior distributions of the first three parameters of the Bayesian hierarchical model. Blue contours indicate the output of PS and black that of a very long SMC run considered as the reference truth.

Table 4: Performance comparison of SMC and PS methods for the Bayesian hierarchical model. The computational cost in terms of the number of likelihood evaluations (calls), the squared bias for the first two posterior moments, and the mean square error (MSE) for the logarithm of the marginal likelihood are presented for varying particle numbers and effective sample size (ESS) fractions ( $\alpha$ ). The values in parentheses denote estimates computed using recycling.

Method	N	$\alpha$	Calls ( $\times 10^6$ )	$b_1^2$	$b_2^2$	$MSE_{\log \mathcal{Z}}$
(R)SMC	64	0.90	0.09	1.7862 (0.6388)	1.8114 (0.5351)	0.53 (0.38)
(R)SMC	128	0.90	0.23	0.4149 (0.1330)	0.3048 (0.0941)	0.21 (0.15)
(R)SMC	256	0.90	0.54	0.0820 (0.0380)	0.0520 (0.0354)	0.06 (0.05)
(R)SMC	64	0.99	0.17	4.7681 (1.5362)	6.9526 (1.7055)	1.30 (0.96)
(R)SMC	128	0.99	0.54	1.3079 (0.3704)	1.2366 (0.2693)	0.72 (0.52)
(R)SMC	256	0.99	1.47	0.1933 (0.0658)	0.1251 (0.0455)	0.32 (0.24)
PS	64	0.90	0.06	0.1478	0.1224	0.08
PS	128	0.90	0.13	0.0667	0.0675	0.04
PS	256	0.90	0.27	0.0248	0.0283	0.02
PS	512	0.90	0.55	0.0087	0.0091	0.01
PS	1024	0.90	1.15	0.0050	0.0055	<0.01
PS	64	0.99	0.07	0.1436	0.1209	0.09
PS	128	0.99	0.15	0.0572	0.0517	0.05
PS	256	0.99	0.31	0.0296	0.0305	0.02
PS	512	0.99	0.63	0.0145	0.0161	0.01
PS	1024	0.99	1.28	0.0042	0.0046	<0.01
PS	64	2.00	0.08	0.0771	0.0772	0.08
PS	128	2.00	0.18	0.0492	0.0522	0.05
PS	256	2.00	0.38	0.0224	0.0274	0.02
PS	512	2.00	0.77	0.0087	0.0102	0.01

The BHM experiment demonstrates PS's effectiveness in handling complex, funnel-like posterior geometries. Table 4 shows PS achieving significantly lower squared bias in posterior moment estimation and marginal likelihood MSE compared to SMC, despite using fewer computational resources. PS's persistent particle strategy enables comprehensive exploration of the posterior landscape, addressing challenges posed by the hierarchical structure and allowing accurate inferences across global and local parameters. Table 4 reinforces the advantage of increasing N over  $\alpha$  for accurate inferences in both posterior and evidence quantities. While recycling reduces  $b_i^2$  for SMC, it appears less effective in improving  $MSE_{\log \mathcal{Z}}$ . PS, on the other hand, maintains a balanced improvement across all metrics as  $N$  increases, suggesting a more holistic exploration

of the posterior landscape. This behavior underscores PS’s potential for providing reliable inferences with fewer particles, a crucial advantage in computationally intensive hierarchical models where increasing  $N$  may be prohibitively expensive.

Fig. 9 illustrates PS’s higher sampling efficiency compared to SMC across all configurations, for both posterior moment estimation and log evidence approximation. Recycling (RSMC) provides only marginal improvements. The performance gap between PS and SMC is particularly pronounced for smaller particle numbers, suggesting PS’s robustness in resource-constrained scenarios. The consistent performance of PS across different  $\alpha$  values (0.90, 0.99, and 2.00) demonstrates its stability and reduced sensitivity to this tuning parameter compared to SMC.

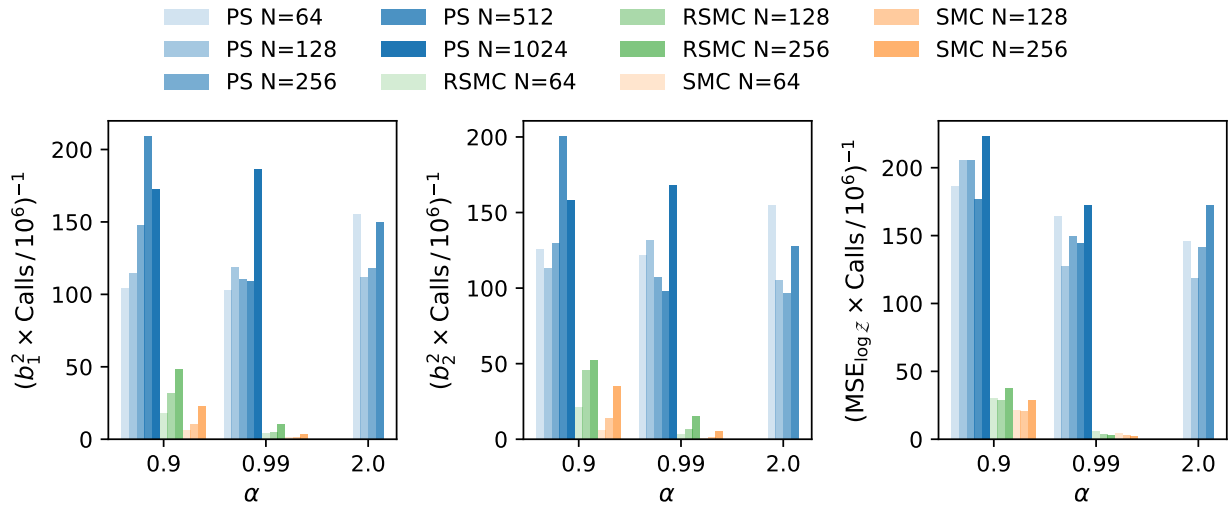


Figure 9: Sampling efficiency for the first (*left*) and second (*middle*) posterior moments (with recycling for SMC) and log model evidence (*right*) for the Bayesian hierarchical model target. Efficiency is quantified as the reciprocal of the product of the metric (e.g.,  $b_1^2$ ,  $b_2^2$ , or  $MSE_{\log \mathcal{Z}}$ ) and the number of likelihood evaluations (Calls). Higher values of efficiency indicate better performance. Configurations of SMC and PS are grouped based on their effective sample size (ESS) fraction ( $\alpha$ ) and represented by varying colors according to the number of particles ( $N$ ).

## 5 Discussion

The numerical experiments presented in Section 4 highlight the significant advantages of the proposed *persistent sampling* (PS) algorithm over standard *sequential Monte Carlo* (SMC) methods across a diverse range of challenging target distributions. PS consistently achieved lower squared bias in estimating the first two posterior moments, as well as substantially lower mean squared error in estimating the marginal likelihood, a crucial quantity for model comparison tasks.

A key strength of PS lies in its ability to maintain a large and diverse set of persistent particles throughout the sampling process. By inclusively reweighting and resampling from all previous iterations, PS constructs a richer approximation of the target posterior distribution. This mitigates

the issues of mode collapse and particle impoverishment that can plague standard SMC, particularly when dealing with multimodal, non-convex, or high-dimensional targets using a limited number of particles.

PS also confers substantial variance reduction benefits. As evidenced by the significantly lower marginal likelihood MSE values, PS provides more accurate and stable estimates of this important quantity compared to SMC. This improvement is especially pronounced in challenging scenarios where SMC struggles, such as the Rosenbrock function and the sparse logistic regression examples.

Furthermore, PS's computational efficiency is noteworthy. Despite maintaining a larger set of persistent particles, PS achieves its superior performance while requiring substantially fewer likelihood evaluations than SMC in most cases. Importantly, this translates into PS requiring fewer temperature levels compared to standard SMC, especially in higher-dimensional problems where the number of required temperature levels increases rapidly for SMC. This property of PS is particularly advantageous, as the computational cost of SMC can become prohibitive in such high-dimensional settings due to the need for a large number of temperature levels.

While PS consistently outperformed SMC in the investigated benchmarks, it is important to acknowledge potential limitations. In extremely high-dimensional settings or with highly complex target distributions, the growth in the number of persistent particles may eventually become prohibitive, negating the computational gains. Additionally, the inclusive reweighting strategy could potentially introduce numerical instabilities if the intermediate distributions are not well-chosen or the temperature ladder is too coarse. Gradient based samplers such as Langevin or Hamiltonian Monte Carlo scale better to high dimensions.

Nonetheless, the overall results demonstrate that PS represents a significant advancement in the field of SMC methods, offering a more robust and efficient sampling algorithm for challenging Bayesian inference problems. By addressing the limitations of standard SMC, PS paves the way for tackling increasingly complex computational tasks arising in various scientific and engineering domains.

Looking ahead, several promising research directions emerge. Investigating alternative reweighting and resampling strategies within the PS framework could further enhance its performance and numerical stability. Additionally, the interplay between PS and modern machine learning techniques, such as normalizing flows or neural networks, presents exciting opportunities for developing more sophisticated and adaptive transition kernels. Furthermore, investigating the use of different Markov transition kernels within the PS framework presents another interesting avenue. In particular, exploring gradient-based kernels could unlock PS's potential in high-dimensional settings where gradient information is available. PS is also compatible with the waste-free SMC framework (Dau and Chopin, 2022). One could imagine a PS algorithm where, in each iteration, one resamples  $N$  particles out of  $(t - 1) \times N \times M$  potential candidates, where  $M$  is the length of the Markov chains.

Moreover, an intriguing connection between PS and *nested sampling* (NS) has emerged. NS

is a Bayesian computation technique that calculates the evidence by transforming the multi-dimensional evidence integral into a single dimension, which is then evaluated numerically using a simple sampling approach (Skilling, 2004, 2006). When setting the number of particles in PS to  $N = 1$  but the ESS fraction  $\alpha$  to a value larger than 1 (e.g.,  $\alpha = 1000$ ), combined with a likelihood-threshold-based annealing scheme, PS appears to reduce to a Monte Carlo version of NS that does not share some of its usual limitations. These include the requirement for independent samples and the reliance on numerical trapezoid rules for evidence estimation. Exploring this avenue further could pave the way for developing new NS methods with superior theoretical properties and sampling performance.

In conclusion, PS, represents a significant methodological advancement in the field of particle-based sampling algorithms. The ability of PS to maintain a diverse and informative set of persistent particles throughout the sampling process leads to more accurate posterior characterization and marginal likelihood estimation while improving computational efficiency. By overcoming the limitations of standard SMC methods, PS offers a powerful tool for researchers and practitioners facing challenging Bayesian inference problems across various scientific and engineering disciplines.

## Acknowledgements

This project has received funding from the U.S. Department of Energy, Office of Science, Office of Advanced Scientific Computing Research under Contract No. DE-AC02-05CH11231 at Lawrence Berkeley National Laboratory to enable research for Data-intensive Machine Learning and Analysis. The authors thank Victor Elvira, Christophe Andrieu, Nicolas Chopin, Michael Williams, Richard Grumitt, and Denja Vaso for helpful discussions.

## References

Nicolas Chopin. A sequential particle filter method for static models. *Biometrika*, 89(3):539–552, 2002.

Pierre Del Moral, Arnaud Doucet, and Ajay Jasra. Sequential monte carlo samplers. *Journal of the Royal Statistical Society Series B: Statistical Methodology*, 68(3):411–436, 2006.

Nicolas Chopin and Omiros Papaspiliopoulos. *An introduction to sequential Monte Carlo*, volume 4. Springer, 2020.

Olivier Cappé, Simon J Godsill, and Eric Moulines. An overview of existing methods and recent advances in sequential monte carlo. *Proceedings of the IEEE*, 95(5):899–924, 2007.

Radford M Neal. Annealed importance sampling. *Statistics and computing*, 11:125–139, 2001.

Nicholas Metropolis, Arianna W Rosenbluth, Marshall N Rosenbluth, Augusta H Teller, and Edward Teller. Equation of state calculations by fast computing machines. *The journal of chemical physics*, 21(6):1087–1092, 1953.

Anthony Lee, Christopher Yau, Michael B Giles, Arnaud Doucet, and Christopher C Holmes. On the utility of graphics cards to perform massively parallel simulation of advanced monte carlo methods. *Journal of computational and graphical statistics*, 19(4):769–789, 2010.

Eric Veach and Leonidas J Guibas. Optimally combining sampling techniques for monte carlo rendering. In *Proceedings of the 22nd annual conference on Computer graphics and interactive techniques*, pages 419–428, 1995.

Eric Veach. *Robust Monte Carlo methods for light transport simulation*. Stanford University, 1998.

Art Owen and Yi Zhou. Safe and effective importance sampling. *Journal of the American Statistical Association*, 95(449):135–143, 2000.

Tim Hesterberg. Weighted average importance sampling and defensive mixture distributions. *Technometrics*, 37(2):185–194, 1995.

Monica F Bugallo, Victor Elvira, Luca Martino, David Luengo, Joaquin Miguez, and Petar M Djuric. Adaptive importance sampling: The past, the present, and the future. *IEEE Signal Processing Magazine*, 34(4):60–79, 2017.

Jean-Marie Cornuet, Jean-Michel Marin, Antonietta Mira, and Christian P Robert. Adaptive multiple importance sampling. *Scandinavian Journal of Statistics*, 39(4):798–812, 2012.

Víctor Elvira, Luca Martino, David Luengo, and Mónica F Bugallo. Improving population monte carlo: Alternative weighting and resampling schemes. *Signal Processing*, 131:77–91, 2017.

Víctor Elvira and Emilie Chouzenoux. Optimized population monte carlo. *IEEE Transactions on Signal Processing*, 70:2489–2501, 2022.

Hai-Dang Dau and Nicolas Chopin. Waste-free sequential monte carlo. *Journal of the Royal Statistical Society Series B: Statistical Methodology*, 84(1):114–148, 2022.

Thi Le Thu Nguyen, Francois Septier, Gareth W Peters, and Yves Delignon. Improving smc sampler estimate by recycling all past simulated particles. In *2014 IEEE Workshop on Statistical Signal Processing (SSP)*, pages 117–120. IEEE, 2014.

Edwin T Jaynes. *Probability theory: The logic of science*. Cambridge university press, 2003.

David JC MacKay. *Information theory, inference and learning algorithms*. Cambridge university press, 2003.

Augustine Kong, Jun S Liu, and Wing Hung Wong. Sequential imputations and bayesian missing data problems. *Journal of the American statistical association*, 89(425):278–288, 1994.

Ajay Jasra, David A Stephens, Arnaud Doucet, and Theodoros Tsagaris. Inference for lévy-driven stochastic volatility models via adaptive sequential monte carlo. *Scandinavian Journal of Statistics*, 38(1):1–22, 2011.

George B Arfken, Hans J Weber, and Frank E Harris. *Mathematical methods for physicists: a comprehensive guide*. Academic press, 2011.

Pierre Del Moral, Arnaud Doucet, and Ajay Jasra. On adaptive resampling strategies for sequential Monte Carlo methods. *Bernoulli*, 18(1):252 – 278, 2012.

Alexandros Beskos, Ajay Jasra, Nikolas Kantas, and Alexandre Thiery. On the convergence of adaptive sequential Monte Carlo methods. *The Annals of Applied Probability*, 26(2):1111 – 1146, 2016.

Tiancheng Li, Miodrag Bolic, and Petar M Djuric. Resampling methods for particle filtering: classification, implementation, and strategies. *IEEE Signal processing magazine*, 32(3):70–86, 2015.

Mathieu Gerber, Nicolas Chopin, and Nick Whiteley. Negative association, ordering and convergence of resampling methods. *The Annals of Statistics*, 47(4):2236–2260, 2019.

Ulf Grenander and Michael I Miller. Representations of knowledge in complex systems. *Journal of the Royal Statistical Society: Series B (Methodological)*, 56(4):549–581, 1994.

Peter J Rossky, Jimmie D Doll, and Harold L Friedman. Brownian dynamics as smart monte carlo simulation. *The Journal of Chemical Physics*, 69(10):4628–4633, 1978.

Gareth O Roberts and Richard L Tweedie. Exponential convergence of langevin distributions and their discrete approximations. *Bernoulli*, pages 341–363, 1996.

Gareth O Roberts and Jeffrey S Rosenthal. Optimal scaling of discrete approximations to langevin diffusions. *Journal of the Royal Statistical Society: Series B (Statistical Methodology)*, 60(1):255–268, 1998.

Simon Duane, Anthony D Kennedy, Brian J Pendleton, and Duncan Roweth. Hybrid Monte Carlo. *Physics letters B*, 195(2):216–222, 1987.

Radford M Neal. MCMC using Hamiltonian dynamics. In *Handbook of Markov Chain Monte Carlo*, pages 113–162. Chapman and Hall/CRC, 2011.

Radford M Neal. Slice sampling. *The annals of statistics*, 31(3):705–767, 2003.

Leah F South, Anthony N Pettitt, and Christopher C Drovandi. Sequential Monte Carlo Samplers with Independent Markov Chain Monte Carlo Proposals. *Bayesian Analysis*, 14(3):753 – 776, 2019.

Minas Karamanis, Florian Beutler, John A Peacock, David Nabergoj, and Uroš Seljak. Accelerating astronomical and cosmological inference with preconditioned monte carlo. *Monthly Notices of the Royal Astronomical Society*, 516(2):1644–1653, 2022.

Robert H Swendsen and Jian-Sheng Wang. Replica monte carlo simulation of spin-glasses. *Physical review letters*, 57(21):2607, 1986.

Charles J Geyer et al. Computing science and statistics: Proceedings of the 23rd symposium on the interface. *American Statistical Association, New York*, 156, 1991.

Robert Gramacy, Richard Samworth, and Ruth King. Importance tempering. *Statistics and Computing*, 20:1–7, 2010.

Axel Finke. *On extended state-space constructions for Monte Carlo methods*. PhD thesis, University of Warwick, 2015.

Víctor Elvira, Luca Martino, David Luengo, and Mónica F Bugallo. Generalized multiple importance sampling. 2019.

Pierre Moral. *Feynman-Kac formulae: genealogical and interacting particle systems with applications*. Springer, 2004.

Matthew D Hoffman and Pavel Sountsov. Tuning-free generalized hamiltonian monte carlo. In *International conference on artificial intelligence and statistics*, pages 7799–7813. PMLR, 2022.

Howard H Rosenbrock. An automatic method for finding the greatest or least value of a function. *The computer journal*, 3(3):175–184, 1960.

Dheeru Dua and Casey Graff. UCI machine learning repository. 2017.

Carlos M Carvalho, Nicholas G Polson, and James G Scott. Handling sparsity via the horseshoe. In *Artificial intelligence and statistics*, pages 73–80. PMLR, 2009.

Andrew Gelman, John B Carlin, Hal S Stern, and Donald B Rubin. *Bayesian data analysis*. Chapman and Hall/CRC, 1995.

Omriros Papaspiliopoulos, Gareth O. Roberts, and Martin Sköld. A general framework for the parametrization of hierarchical models. *Statistical Science*, 22(1):59–73, 2007. ISSN 08834237.

John Skilling. Nested sampling. *Bayesian inference and maximum entropy methods in science and engineering*, 735:395–405, 2004.

John Skilling. Nested sampling for general bayesian computation. 2006.